BAW-10174

Topical Report
Revision 1
November 1990

Mark-BW Reload LOCA Analysis for the Catawba and McGuire Units

Babcock & Wilcox Fuel Company
P. O. Box 10935
Lynchburg, Virginia 24506-0935

Babcock & Wilcox Fuel Company
P. O. Box 10935
Lynchburg, Virginia 24506-0935

Topical Report BAW-10174

Revision 1
November 1990

Mark-BW Reload LOCA Analysis

for the

Catawba and McGuire Units

Key Words: Large Break, LOCA, Transient, Water Reactors

ABSTRACT

The B&W Fuel Company will be delivering reload fuel to the Duke Power Catawba and McGuire Units beginning in 1991. This report presents a complete LOCA evaluation for operation of the Catawba and McGuire nuclear units with Mark-BW reload fuel. Compliance with the criteria of 10 CFR 50.46 is demonstrated. Operation of the units while in transition from Westinghouse-supplied OFA fuel to B&W-supplied Mark-BW fuel is also justified. Other B&W topical reports describe the Mark-BW fuel assembly design; the mechanical, nuclear, and thermal-hydraulics methods supporting the design; and ECCS codes and methods. The analyses and evaluations presented in this report serve, in conjunction with the other topical reports, as a reference for future reload safety evaluations applicable to cores with BWFC-supplied fuel assemblies.

ACKNOWLEDGEMENTS

The B&W Fuel Company wishes to acknowledge the efforts put forth by J. R. Biller, J. J. Cudlin, B. M. Dunn, J. A. Klingenfus, R. J. Lowe, C. K. Nithianandan, N. H. Shah, and K. C. Shieh in preparing and documenting the material contained in this report.

Topical Report Revision Record

Documentation Revision	Description
0	Original issue.
1	Add Appendix B--increased 9.7' case F_q. Correct x-scale on Chapter 8 mass flux plots. NRC requested updates.

TABLE OF CONTENTS

1. Introduction 1.1

2. Summary and Conclusions 2.1

3. Plant Description 3.1
   3.1 Physical Description 3.1
   3.2 Description of Emergency Core Cooling System . . 3.4
   3.3 Plant Parameters 3.5

4. Analysis Inputs and Assumptions 4.1
   4.1 Computer Codes and Methods 4.1
   4.2 Inputs and Assumptions 4.1
      4.2.1 RELAP5/MOD2-B&W Modeling 4.2
      4.2.2 REFLOD3B Modeling 4.7
      4.2.3 FRAP-T6-B&W Modeling 4.9
      4.2.4 BEACH Modeling 4.9
   4.3 Comparison of Plant Model with McGuire & Catawba 4.10

5. Evaluation Model Changes 5.1
   5.1 Revisions to the BWFC LOCA Evaluation Model. . . 5.2
   5.2 Effects of Evaluation Model Revisions 5.4

6. Sensitivity Studies 6.1
   6.1 Evaluation Model Generic Studies 6.1
   6.2 Confirmable Sensitivity Studies 6.5
   6.3 Break Location 6.11

7. Plant-Specific Studies and Spectrum Analysis 7.1
7.1 Base Case 7.1
7.2 Accumulator Configuration 7.2
7.3 Break Spectrum Analysis 7.3
7.4 Break Type 7.5
7.5 Maximum ECCS Analysis 7.7

8. LOCA Limits 8.1
8.1 LOCA Limits Dependencies 8.1
8.2 LOCA Limits Calculation Results 8.3
8.3 Compliance to 10 CFR 50.46 . . . . . 8.6.1

9. Whole-Core Oxidation and Hydrogen Generation 9.1

10. Core Geometry 10.1

11. Long-Term Cooling 11.1
11.1 Initial Cladding Cooldown 11.1
11.2 Extended Coolant Supply 11.2
11.3 Boric Acid Concentration 11.2
11.4 Adherence to Long-Term Cooling Criteria 11.4

12. Small Break LOCA 12.1
12.1 SBLOCA Transient 12.1
12.2 Fuel Design Effects 12.4
12.3 Current FSAR Results 12.7
12.4 Compliance with Acceptance Criteria 12.7

13. References 13.1

Appendix A. Evaluation of Transition Cores . . . . A 1
A.1 OFA and Mark-BW Design Differences A.1
A.2 Assessment of Impact on Peak Cladding Temperatures A.3
A.3 Conclusions A.6

Appendix B. F_q Increase--9.7' LOCA Limits Case . . B.1 |

List of Tables

Table		Page
2-1	Summary of Results (LOCA Limit Runs)	2.3
3-1	Plant Parameters and Operating Conditions . .	3.6
4-1	Comparison of LOCA Model Geometric Values to Plant FSAR Data	4.14
7-1	Spectrum and Break Type Comparison	7.9
8-1	LOCA Limits Results	8.7
A-1	OFA / Mark-BW Design Differences	A.7
B-1	LOCA Limits Results--Updated 9.7' Case . . .	B.3

List of Figures

Figure		Page
4-1	Large Break Analysis Code Interface	4.16
4-2a	RELAP5/MOD2-B&W LBLOCA Noding Diagram Reactor Coolant Loops	4.17
4-2b	RELAP5/MOD2-B&W LBLOCA Noding Diagram Reactor Core	4.18
4-3	REFLOD3B Noding Diagram	4.19
4-4	BEACH and FRAP-T6-B&W Noding Diagram for Mark-BW Fuel Assembly	4.20
5-1	Revision 0 Evaluation Model Code Interfaces for Large Break LOCA	5.9
6-1	Core Mass Flux for EM Spectrum Study Versus McGuire/Catawba Base Model . . .	6.13
6-2	TACO3 Fuel Temperatures as a Function of Burnup	6.13
7-1	Plant-specific Studies Analysis Diagram . . .	7.10
7-2	Sensitivity Study - Base Model System Pressure During Blowdown	7.11
7-3	Sensitivity Study - Base Model Mass Flux During Blowdown at Peak Power Location	7.11
7-4	Sensitivity Study - Base Model Reflooding Rate	7.12
7-5	Sensitivity Study - Base Model Heat Transfer Coefficient at Peak Power Location	7.12
7-6	Sensitivity Study - Base Model Peak Cladding Temperature	7.13
7-7	Sensitivity Study - Base Model Cladding Temperature at Rupture Location	7.13
7-8	Sensitivity Study - Base Model Cladding Temperature in Adjacent Grid Span , ...	7.14
7-9a	Sensitivity Study - Base Model Fluid Temperature at PCT Location	7.14
7-9b	Sensitivity Study - Base Model Fluid Temperature at PCT Location	7.15

List of Figures (Con't)

Figure		Page
8-5	LOCA Limits Study - 2.9 Foot Case Cladding Temperatures	8.10
8-6	LOCA Limits Study - 2.9 Foot Case Heat Transfer Coefficient at PCT Location	8.10
8-7	LOCA Limits Study - 2.9 Foot Case Local Oxidation	8.11
8-8	LOCA Limits Study - 4.6 Foot Case Mass Flux During Blowdown at Peak Power Location	8.11
8-9	LOCA Limits Study - 4.6 Foot Case Cladding Temperatures	8.12
8-10	LOCA Limits Study - 4.6 Foot Case Heat Transfer Coefficient at PCT Location	8.12
8-11	LOCA Limits Study - 4.6 Foot Case Local Oxidation	8.13
8-12	LOCA Limits Study - 6.3 Foot Case Mass Flux During Blowdown at Peak Power Location	8.13
8-13	LOCA Limits Study - 6.3 Foot Case Cladding Temperatures	8.14
8-14	LOCA Limits Study - 6.3 Foot Case Heat Transfer Coefficient at PCT Location	8.14
8-15	LOCA Limits Study - 6.3 Foot Case Local Oxidation	8.15
8-16	LOCA Limits Study - 8.0 Foot Case Mass Flux During Blowdown at Peak Power Location	8.15
8-17	LOCA Limits Study - 8.0 Foot Case Cladding Temperatures	8.16
8-18	LOCA Limits Study - 8.0 Foot Case Heat Transfer Coefficient at PCT Location	8.16
8-19	LOCA Limits Study - 8.0 Foot Case Local Oxidation	8.17
8-20	LOCA Limits Study - 9.7 Foot Case Mass Flux During Blowdown at Peak Power Location	8.17

List of Figures (Con't)

Figure		Page
8-21	LOCA Limits Study - 9.7 Foot Case Cladding Temperatures	8.18
8-22	LOCA Limits Study - 9.7 Foot Case Heat Transfer Coefficient at PCT Location	8.18
8-23	LOCA Limits Study - [illegible]ot Case Local Oxidation	8.19
B-1	Axial Dependence o[illegible] Total Peaking Factor Large Break[illegible]rk-BW, Updated 9.7 Foot Case	B.4
B-2	LOCA Limit Study - Axial Power S[illegible] Updated 9.7 Foot Case	B.4
B-3	LOCA Limits Study - Upd[illegible].7 Foot Case Mass Flux During Blowdown [illegible]c Peak Power Location	B.5
B-4	LOCA Limits Study - Updated 9.7 Foot Case Cladding Temperatures	B.5
B-5	LOCA Limits Study - Updated 9.7 Foot Case Heat Transfer Coefficient at PCT Location . .	B.6
B-6	LOCA Limits Study - Updated 9.7 Foot Case Local Oxidation	B.6

Table 2-1 Summary of Results (LOCA Limit Runs)

Core Elevation, ft	Peak Cladding Temperature, F[1]	Maximum Oxidation, % Local	Maximum Oxidation, % Whole Core
2.9	1816	3.4	0.25
4.6	1963	5.2	0.41[2]
6.3	1873	4.8	0.40
8.0	1930	4.7	0.32
9.7[3]	1823	3.7	0.29

1 See the response to question number 30 on BAW-10174 and the response to question 5 on BAW-10166, Revision 2.

2 See the response to question number 13 on BAW-10174 and the response to question number 2 on BAW-10168, Revision 1.

3 See Appendix B (reanalysis of the 9.7' case at a higher F_q).

8. LOCA Limits

The LOCA evaluation is completed with a set of analyses done to show compliance with 10 CFR 50.46 for the core power and peaking that will be taken as the limiting LOCA conditions for core operation, that is, the LOCA limits. The term limit is applied because these cases are run at the limit of allowable local power operation. Actually, these LOCA evaluations serve as the bases for the allowable local power. As such, the LOCA limits calculations comprise the cases that are used to demonstrate compliance of the reload fuel cycles and peaking limits to the criteria of 10 CFR 50.46. Five runs are made at differing axial elevations such that a curve of allowable peak linear heat rates as a function of elevation in the core can be constructed or, in this case, confirmed. This curve becomes a part of the plant technical specifications, and plant operation is controlled such that the local peaking and power do not exceed the allowable values. (Note: The 9.7' LOCA limits case has been reanalyzed at a higher F_q and the results of the case are reported in Appendix B along with a revised total peaking factor curve, Figure B-1.)

8.1 LOCA Limits Conditions

The absolute LOCA limits to power and peaking for each elevation in the core can be determined through repeated calculations at each elevation, with successively higher local power levels, until the analysis shows one or more of the applicable acceptance criteria to be exceeded. The highest linear heat rate for which the criteria are not exceeded is the absolute LOCA limit for a particular elevation. The more practical approach, the one adopted for this report, assumes a set of peaking limits at a given power level that have been determined to be acceptable for fuel cycle design and plant operations purposes. The LOCA limits

analyses are then done to confirm that the assumed limits will meet the applicable criteria.

Figure 8-1 shows the axial power and peaking selected and confirmed as applicable to the McGuire and Catawba plants for operation with Mark-BW fuel. With the axial power and peaking dependency established, LOCA calculations are performed with the core power level and total peaking initialized at different positions on the curve to demonstrate that these peaking limitations assure compliance with 10 CFR 50.46. Should the results not comply, the allowed peaking is reduced, and the analysis is repeated until acceptable results can be obtained. Likewise, if the results show large margins of compliance, the peaking may be increased to provide additional operational flexibility. For these analyses, neither of these steps was taken although the results do show considerable margins at certain elevations.

An additional condition assumed in these analyses is that the allowable peaking will be dependent on fuel assembly burnup in accordance with Figure 8-2. This limitation is made necessary because, at burnups approaching 50000 MWd/MTu, the initial fuel enthalpy and internal pressure can become a more severe combination than the beginning-of-life values. By assuring that the local heating rates will be limited to those shown in Figure 8-2, the reduction in power compensates for the increases in fuel temperature and pin pressure such that the beginning-of-life conditions remain the most severe. (This is discussed in greater detail in the time-in-life sensitivity studies, Section 6.2.) Therefore, Figure 8-2 is a limit of operation for the Mark-BW fuel. The limit is checked during the fuel design process. However, at the high burnup at which the limit is imposed there should be no restrictions on core operation, because the highly

depleted fuel is unlikely to reach the limit within the operational envelopes of the plant Technical Specifications.

8.2 LOCA Limits Results

To validate Figure 8-1, five separate LOCA calculations were performed. Power peaks were run centered at the middle of the second through the sixth grid spans. Figure 8-3 shows the axial power shapes evaluated. For all cases, the radial power peaking was 1.55. The combination of the axial peaking of Figure 8-3 and a 1.55 radial yields the total peaking at the corresponding elevation shown in Figure 8-1.

The results of the calculations are tabulated in Table 8-1 and shown in Figures 8-4 through 8-23. The figures comprise five sets with four figures in each set. The four figures of each set show (1) the mass flux at the elevation of peak power, (2) the cladding temperature for three different locations on the pin, (3) the heat transfer coefficient at the location of highest cladding temperature, and (4) the distribution of cladding oxidation along the pin. Only one mass flux plot is provided for each case because the axial variations in mass flux are not strong. This can be observed by comparing the five mass flux curves for the different peaking cases.

To demonstrate the cladding temperature results, three curves are presented for each case. Temperature histories are shown for the rupture location, for the node adjacent to the rupture, and for the high temperature node in an adjacent grid span. For power distributions peaked toward the middle of the core, rupture location is almost certain to correspond to the location of peak power. Near the time of rupture, the portion of the pin immediately above the rupture site will be at nearly the same temperature. Following rupture, the burst location cools quickly

as the cladding pulls away from the fuel, and the area for heat transfer is increased. Due to axial heat conduction in the cladding and the effect of the rupture on flow conditions, the cooling in the node just above the rupture is substantially improved. This means that although one of the nodes in the adjacent grid span is at a lower power, it can develop as the location of the highest cladding temperature.

The heat transfer coefficient (HTC) is shown for the peak cladding temperature location. HTC variations with elevation are as expected (see Figures 7-51 through 7-53), such that the HTC from one elevation reasonably characterizes the other elevations. The last figure in each set shows the local oxide thickness as a function of elevation for the fuel pin. Each figure shows total oxidation including that assumed prior to the start of the accident. Oxidation up to the time the cladding falls below 1500 F or the elevation has been covered by mixture, as measured by the REFLOD3B core water level, is included. The large variations of the resultant curve reflect the relatively lower cladding oxidation in the vicinity of the grid and rupture locations.

2.9-ft Peak Power Case

In this case, the axial power shape is peaked well below the core midplane, and the cladding temperature responses differ accordingly from those calculated in the 4-,6-, and 8-ft cases. The peak power locations on the rod are cooled rapidly during reflood and have not reached temperatures sufficient to cause a rupture by the time of temperature turnaround. Therefore, the rupture occurs in node 8, the center node of the grid span above the location of peak power. This region of the core is also cooled rapidly, and the peak cladding temperature occurs in the grid span above the ruptured location. Although the power at the midplane is about 80 percent of that at the peak power location,

the central node in the mid-core grid span produces the highest cladding temperature, 1816 F. The highest local oxidation, 3.4 percent, occurs at the ruptured location. The whole core oxidation calculated for this LOCA is 0.25 percent.

4.6-ft Peak Power Case

With the power peaked at 4.6 feet, the cladding temperature responses resemble closely those obtained for the other two mid-core peaks. The rupture occurs at the location of peak power. The node above the rupture experiences increased cooling post rupture, and the peak cladding temperature occurs in the downstream grid span (node 11). The temperature at this location is about 100 F above the temperatures near the rupture location. The highest local oxidation, 5.2 percent, also occurs at the mid-core elevation. The whole core oxidation during this LOCA is 0.41 percent, the highest obtained in the set of LOCA limits analyses.

6.3-ft Peak Power Case

For a peak power situated at the core midplane, the cladding temperature response corresponds to that described in the previous paragraph. The rupture is at the location of peak power. For this case, however, the post rupture cooling axial conduction does not outweigh the effect of the relatively lower power at the next span, and the peak cladding temperature occurs in the node just above the rupture location. As shown in Figure 8-13, the peak temperature, 1873 F, is only slightly higher, by about 70 F, than that predicted for the next higher grid span. The highest local oxidation in this case, 4.8 percent, occurs for the peak cladding temperature node. The whole core oxidation is 0.40 percent.

8.0-ft Peak Power Case

Again, the temperature responses follow the pattern described for the previous two cases. Here, with the power peaked toward the outlet, the grid span that will produce high cladding temperatures lies below the location of peak power. The rupture occurs at the location of peak power and the peak cladding temperature, 1930 F, is predicted to occur in the grid span below the peak location. The markedly higher flow velocities at the higher elevations, in conjunction with rupture cooling effects and the drop-off of power, combine to produce a cladding temperature in the node above the rupture location that is nearly 200 F below the peak cladding temperature (node 12). The highest local oxidation is 4.7 percent, and the whole core oxidation is 0.32 percent.

9.7-ft Peak Power Case

In accordance with the axial dependency of power peaking shown in Figure 8-1, this case is run at a slightly lower total peaking than the other four cases. The location of peak power is in node 17, which experiences some cooling due to grid effects. With the reduction in peaking and the severe outlet shape, the power in node 15 is close to that in node 17. Because the lower location, node 15, is at the end of the grid span, there is little, if any, grid effect. Thus, node 15 is the first location on the fuel pin to reach the rupture temperature. Since the rupture occurs at a node adjacent to the grid span, the rupture and spacer grid effects combine to provide better cooling in a higher powered grid span. The peak temperature, 1823 F, occurs just below the rupture location. The peak local oxidation is 3.7 percent and the whole core oxidation is 0.29 percent. (Note: The 9.7' case has been reanalyzed at a higher F_q and the results of the analysis are reported in Appendix B.)

8.3 Compliance to 10 CFR 50.46

The LOCA limits calculations directly demonstrate compliance to two of the criteria of 10 CFR 50.46 and serve as the basis for demonstrating compliance with two others. As seen in the figures and in Table 8-1, the highest peak cladding temperature, 1963 F, and the highest local oxidation, 5.2 percent, are well below the 2200 F and 17 percent criteria. Chapter 9 documents compliance with the whole core oxidation limit based on the local oxidations calculated for these evaluations, and Chapter 10 documents the core geometry based on the deformations predicted for the LOCA.

Table 8-1 LOCA Limits Results[1]

Item or Parameter	Elevation of Peak Power, Feet 2.9	4.6	6.3	8.0	9.7[2]
End-of-Blowdown, s	21.0	21.3	21.2	20.7	20.8
Liquid in Reactor Vessel at EOB, ft^3	93.1	70.2	71.8	83.9	79.0
Bottom-of-Core Recovery, s	33.0	33.7	33.5	32.8	32.9
Time of Rupture, s	81.8	74.4	67.6	73.8	84.4
Ruptured Node *	8	8	11	14	15
PCT at Rupture Node, F	1611	1669	1666	1655	1602
Oxide at Rupture Node, %	3.4	3.5	4.8	1.5	0.8
Node Adjacent to Rupture *	9	9	12	15	14
PCT of Adjacent Node, F	1804	1839	1873	1753	1823
Oxide at Adjacent Node, %	2.9	3.1	4.4	3.0	3.2
Node in Adjacent Grid Span *	11	11	14	12	12
PCT of Adjacent Grid Span, F	1816	1963	1805	1930	1718
Oxide at Adjacent Grid Span, %	3.0	5.2	3 4	4.7	2.0
Pin PCT Node *	11	11	12	12	14
Peak Local Oxidation, %	3.4	5.2	4.8	4.7	3.7
Whole Core Oxidation, %	0.25	0.41	0.40	0.32	0.29

* Refer to Figure 4-4 for noding arrangement.

1 See the responses to question numbers 13 and 30 on BAW-10174, the response to question number 2 on BAW-10168, Revision 1, and the response to question number 5 on BAW-10166, Revision 2.

2 The 9.7' case has been reanalyzed at a higher F_q and the results of the analysis are reported in Appendix B.

FIGURE 8-1 AXIAL DEPENDENCE OF ALLOWED TOTAL PEAKING FACTOR
LARGE BREAK LOCA MARK-BW

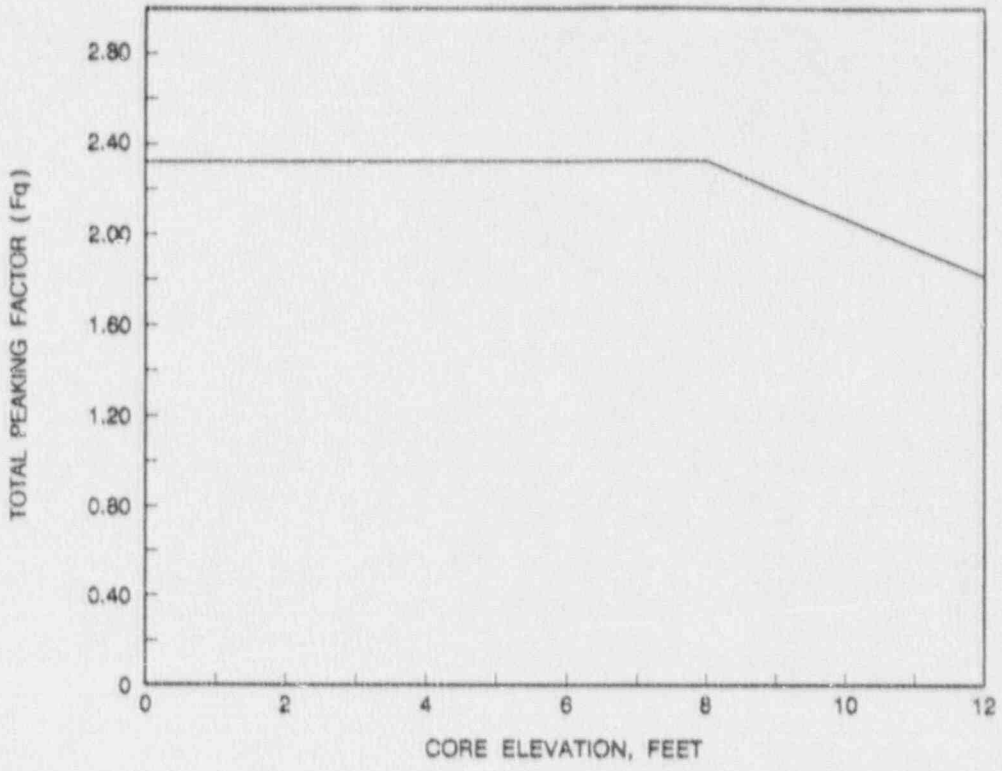

FIGURE 8-2 NORMALIZED LOCAL POWER BURNUP DEPENDENCY FACTOR

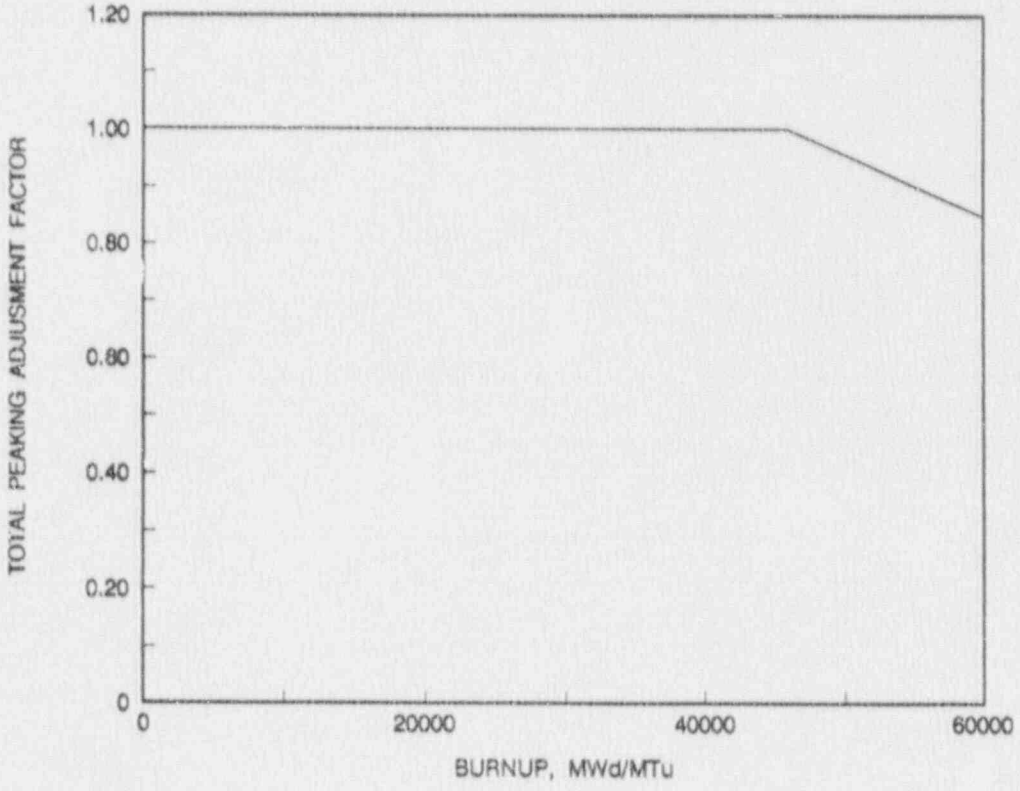

FIGURE 8-3 LOCA LIMIT STUDY - AXIAL POWER SHAPES

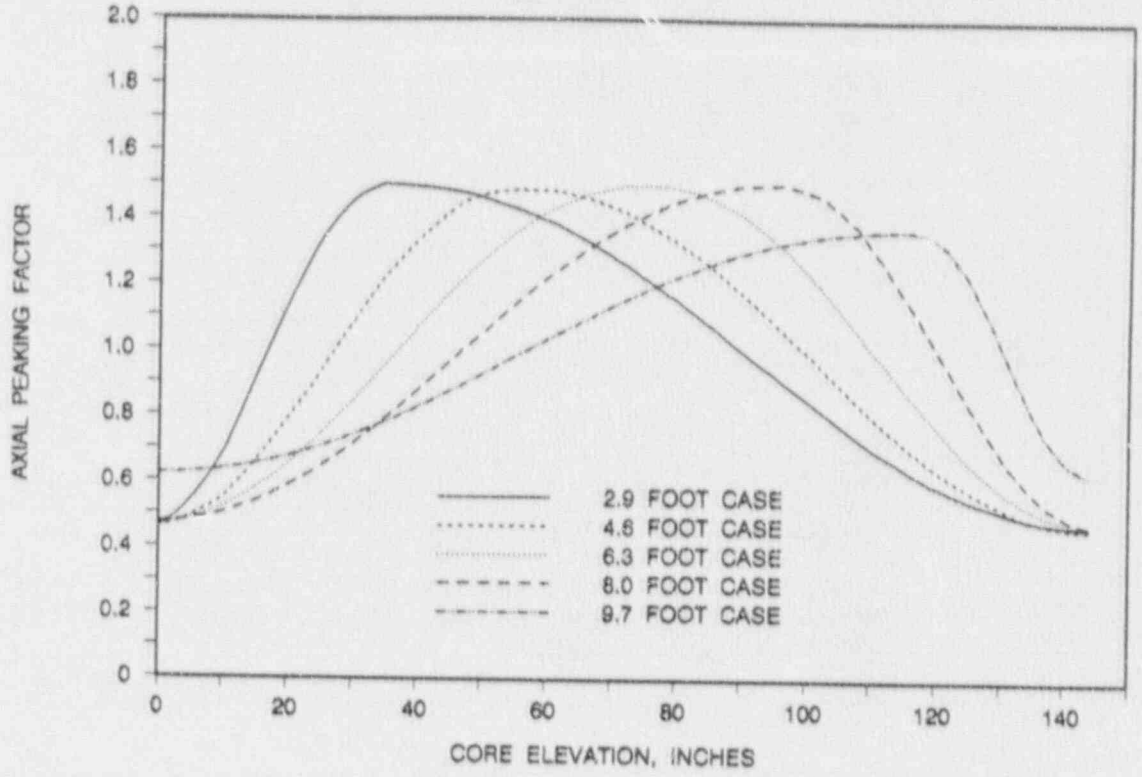

FIGURE 8-4 LOCA LIMITS STUDY - 2.9 FOOT CASE
MASS FLUX DURING BLOWDOWN AT PEAK POWER LOCATION

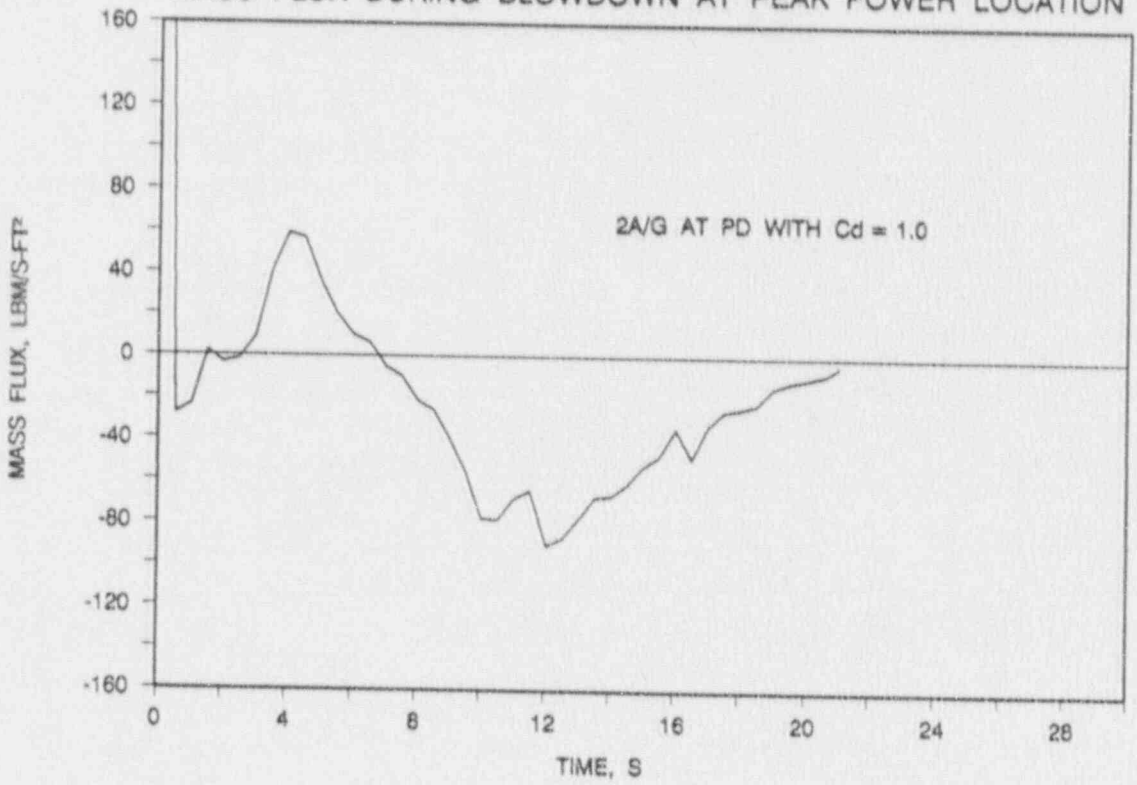

FIGURE 8-5 LOCA LIMITS STUDY - 2.9 FOOT CASE
CLADDING TEMPERATURES

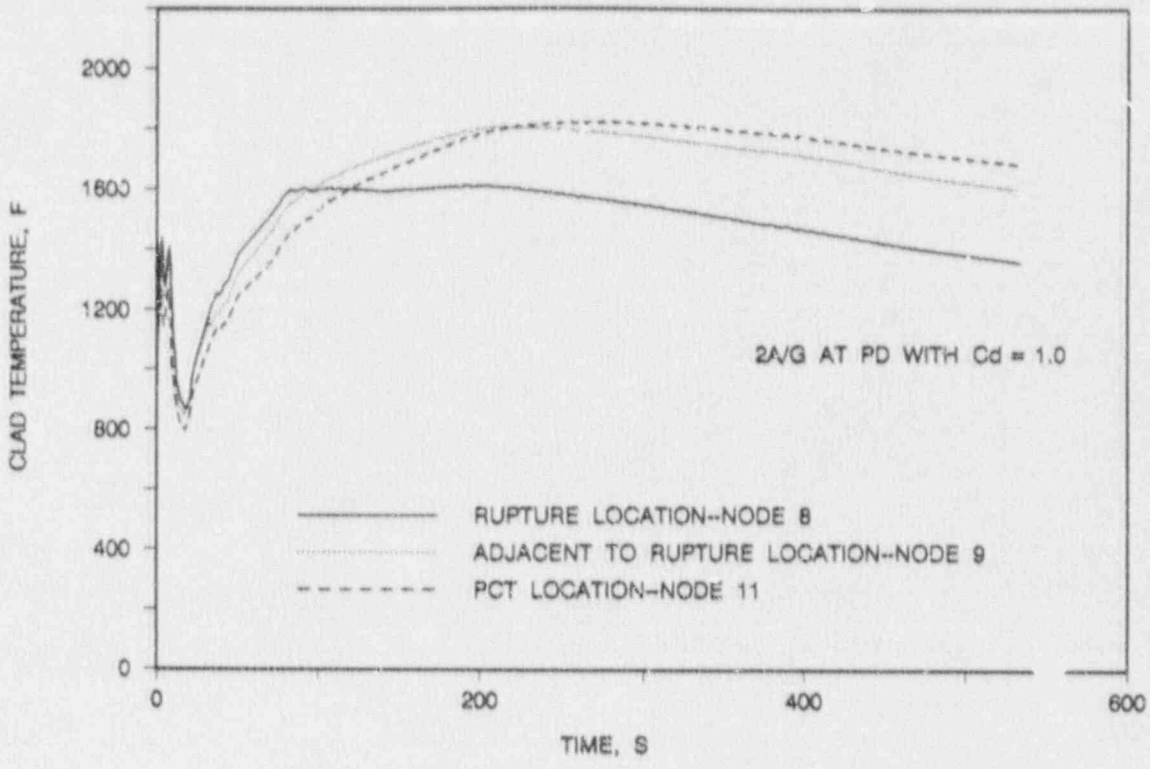

FIGURE 8-6 LOCA LIMITS STUDY - 2.9 FOOT CASE
HEAT TRANSFER COEFFICIENT AT PCT LOCATION

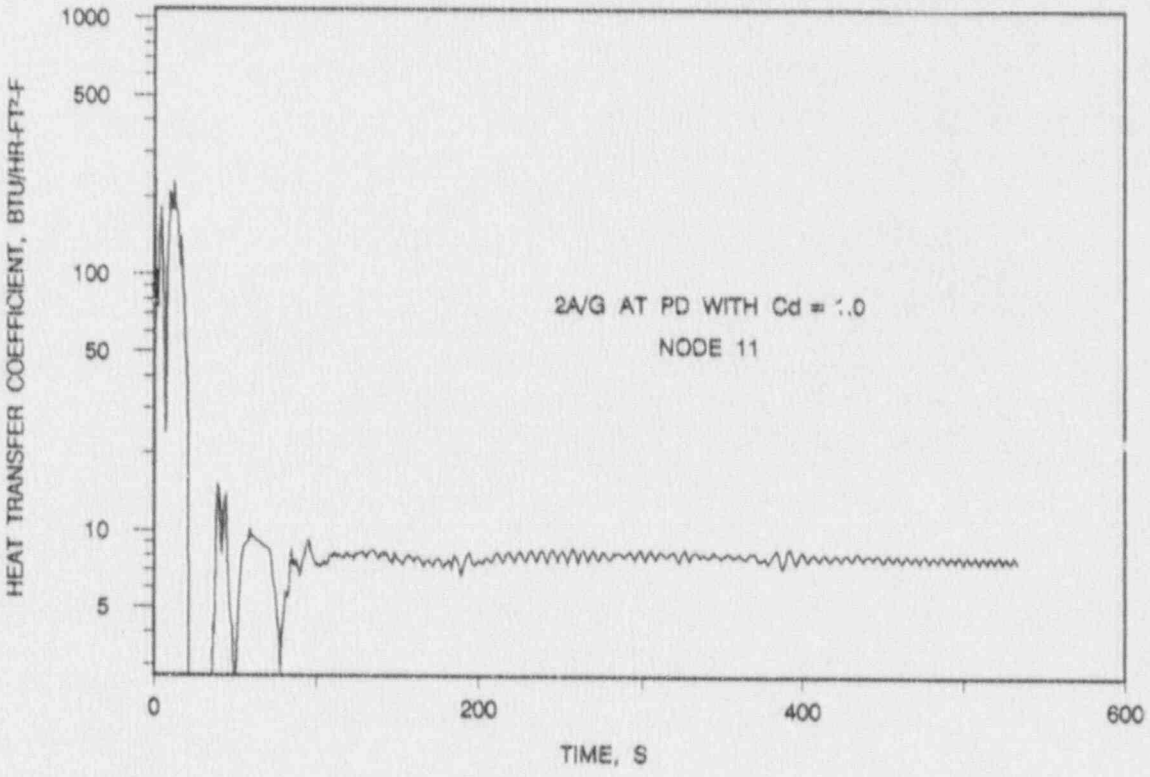

FIGURE 8-7 LOCA LIMITS STUDY - 2.9 FOOT CASE
LOCAL OXIDATION

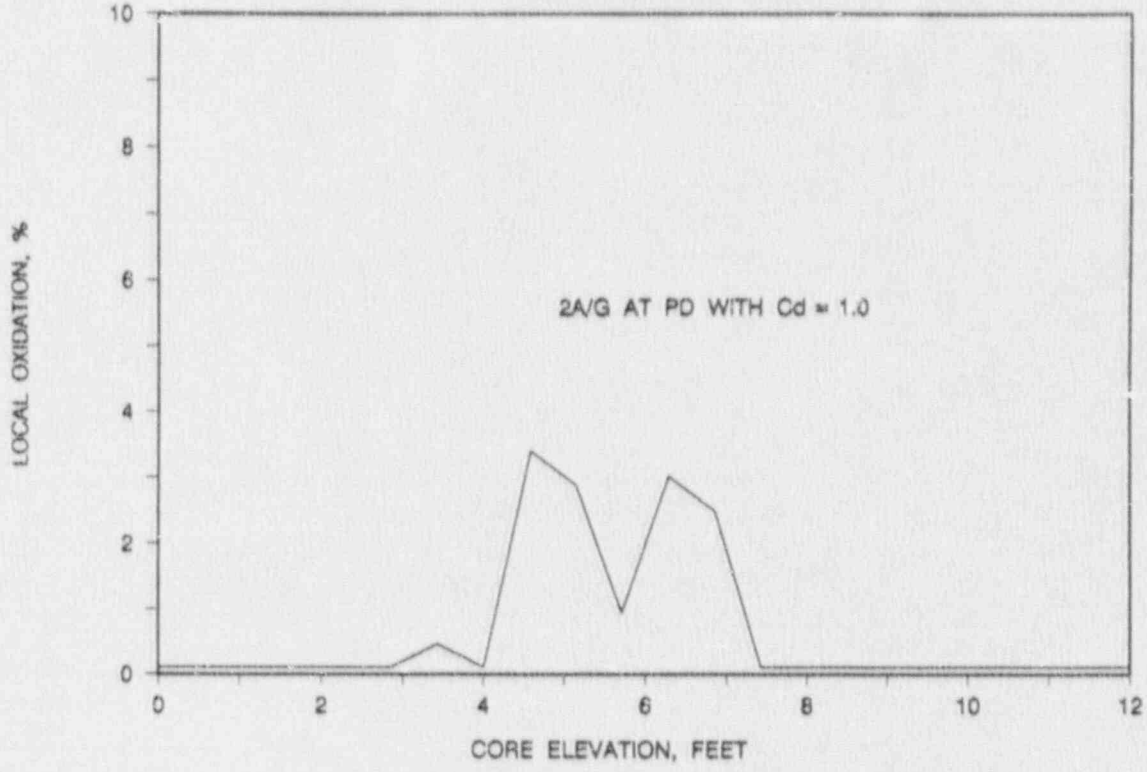

FIGURE 8-8 LOCA LIMITS STUDY - 4.6 FOOT CASE
MASS FLUX DURING BLOWDOWN AT PEAK POWER LOCATION

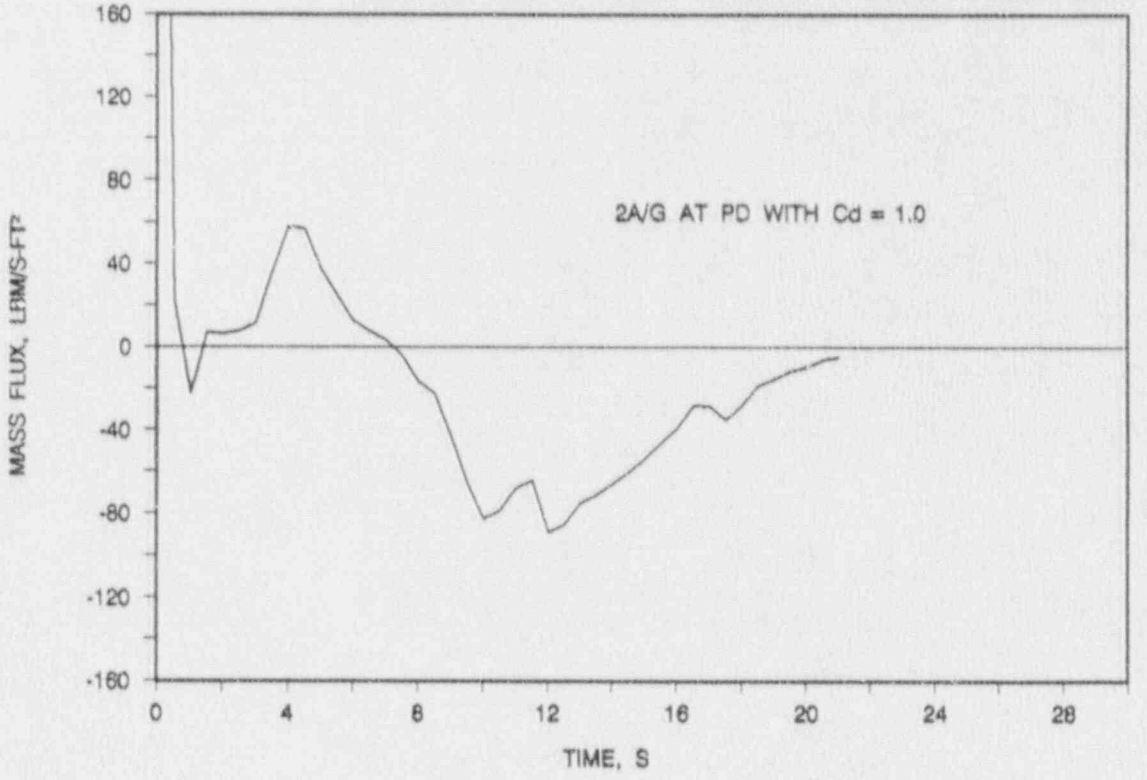

FIGURE 8-9 LOCA LIMITS STUDY - 4.6 FOOT CASE
CLADDING TEMPERATURES

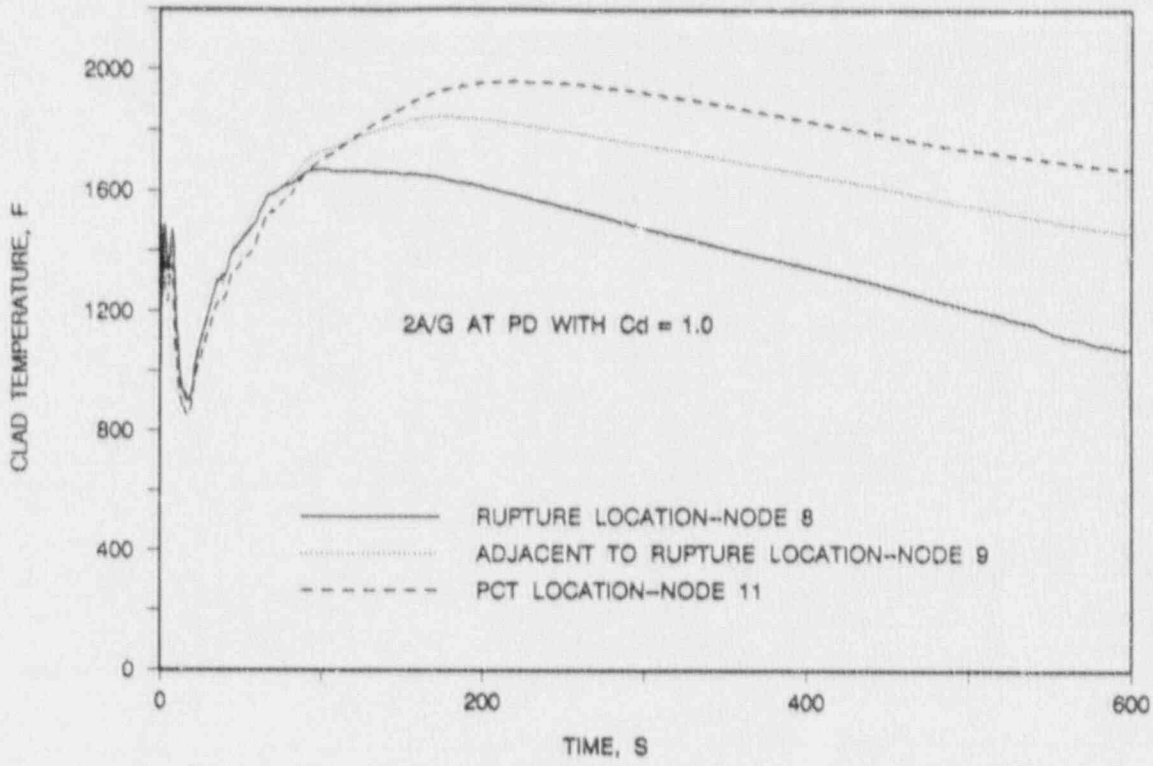

FIGURE 8-10 LOCA LIMITS STUDY - 4.6 FOOT CASE
HEAT TRANSFER COEFFICIENT AT PCT LOCATION

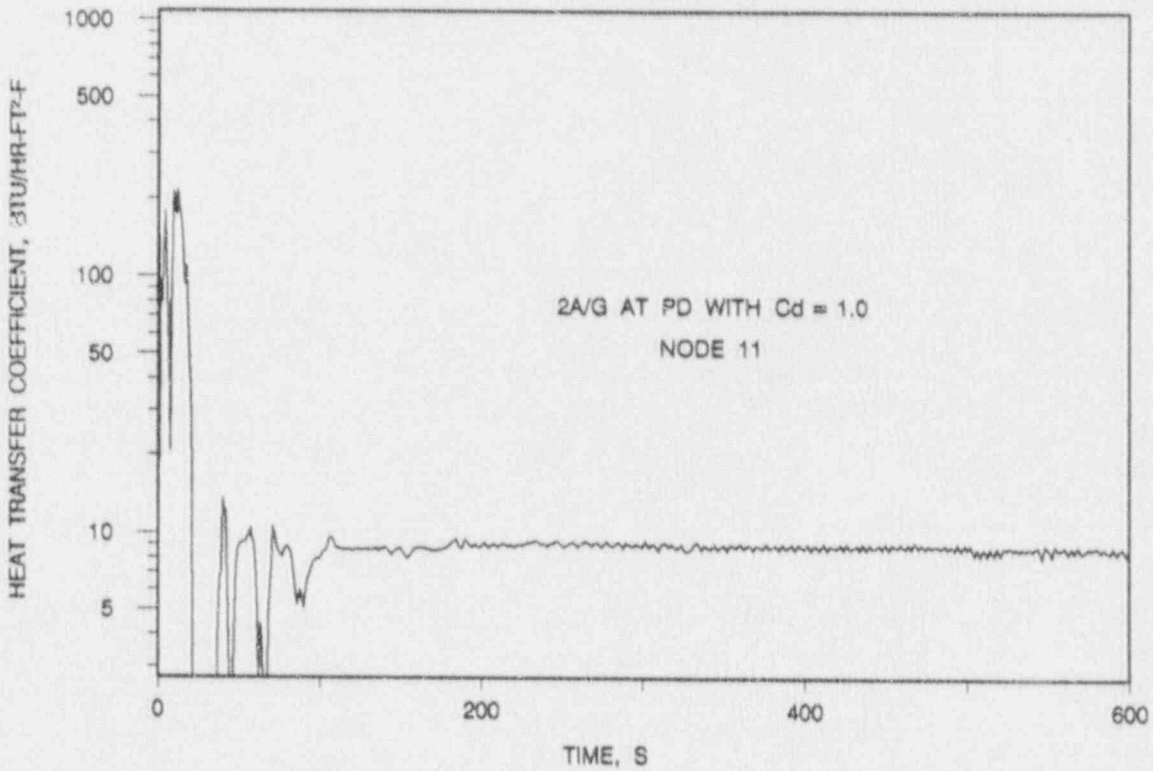

FIGURE 8-11 LOCA LIMITS STUDY - 4.6 FOOT CASE
LOCAL OXIDATION

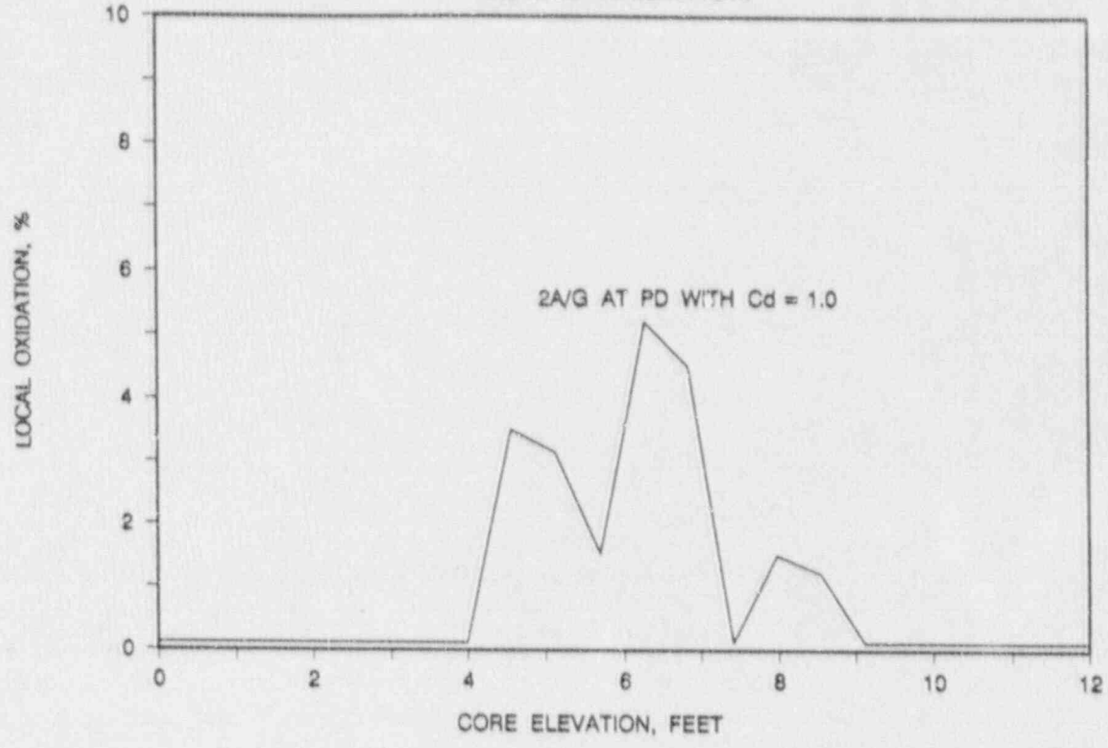

FIGURE 8-12 LOCA LIMITS STUDY - 6.3 FOOT CASE
MASS FLUX DURING BLOWDOWN AT PEAK POWER LOCATION

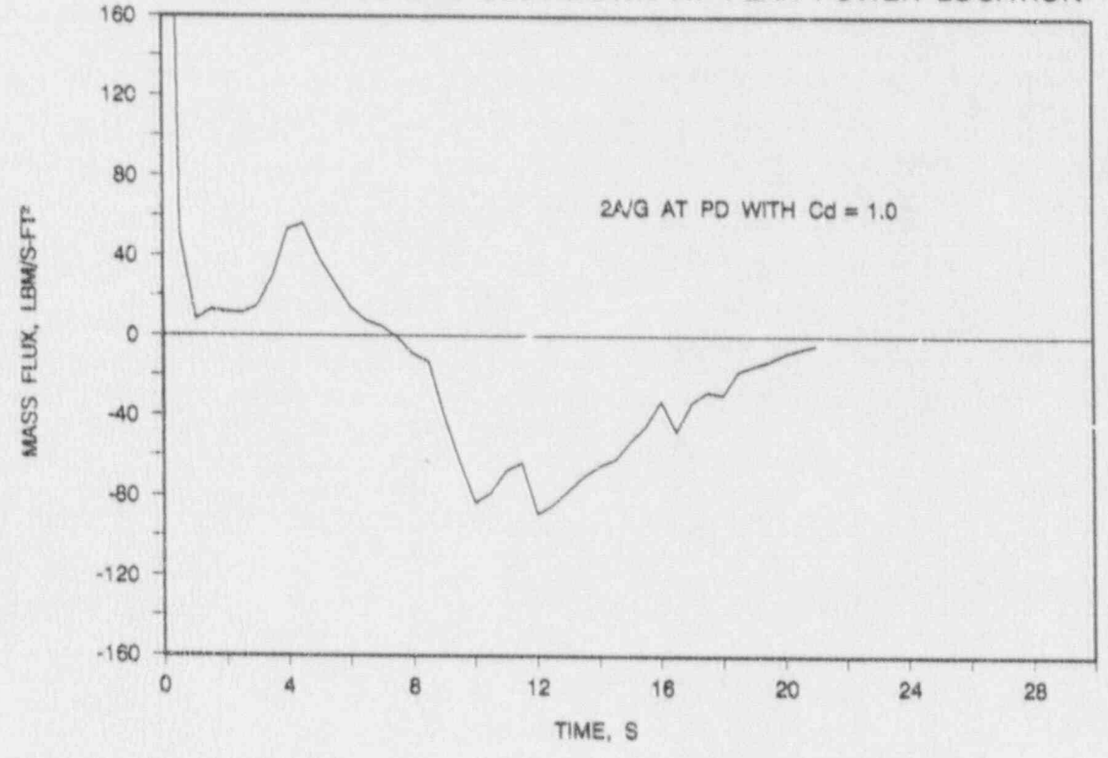

FIGURE 8-13 LOCA LIMITS STUDY - 6.3 FOOT CASE
CLADDING TEMPERATURES

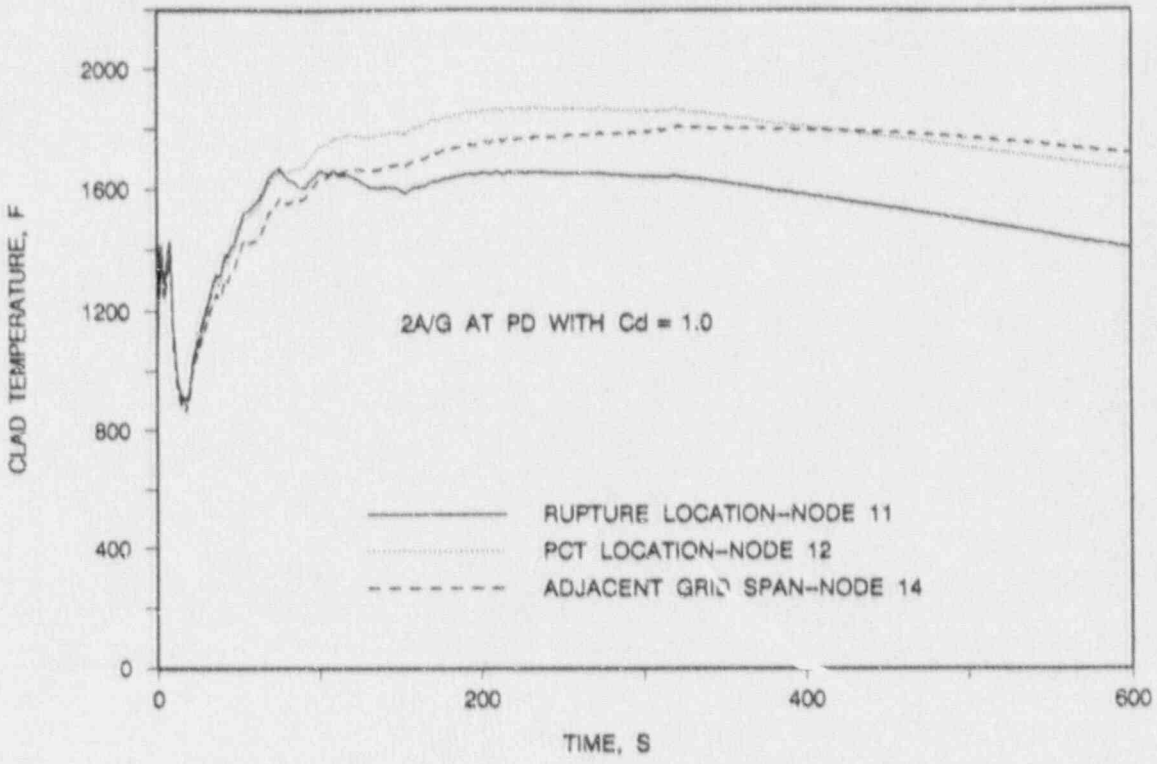

FIGURE 8-14 LOCA LIMITS STUDY - 6.3 FOOT CASE
HEAT TRANSFER COEFFICIENT AT PCT LOCATION

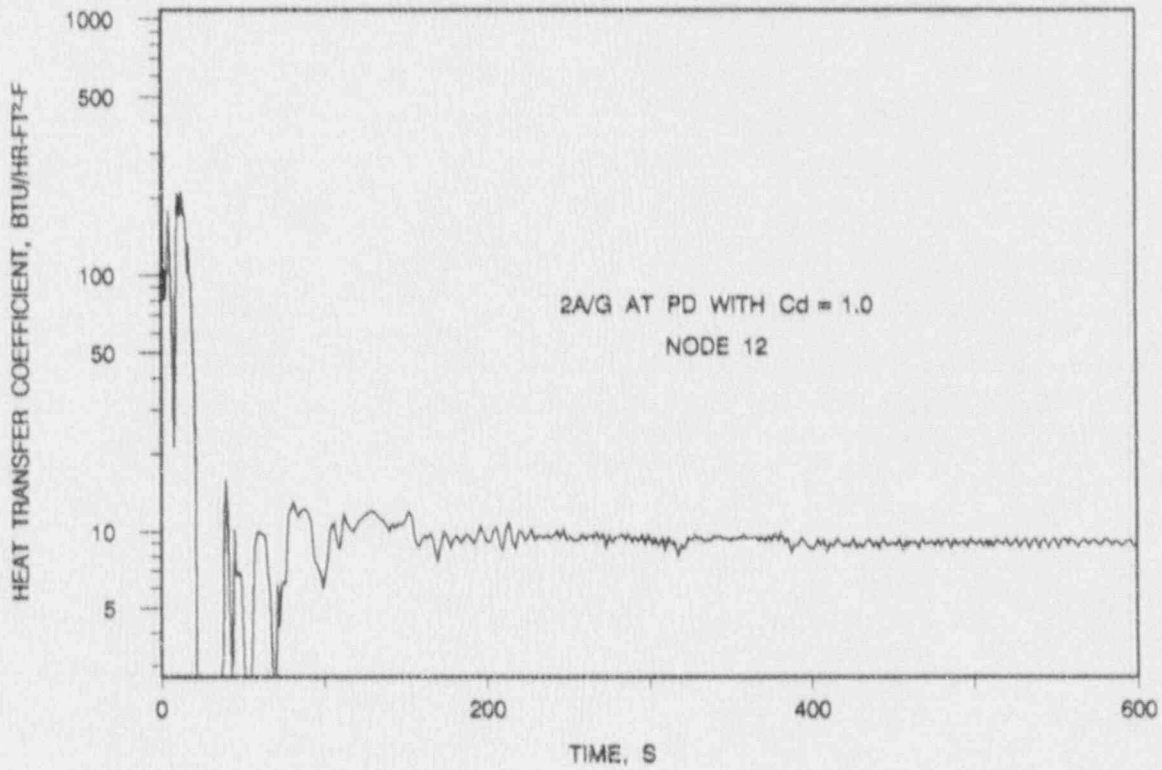

FIGURE 8-15 LOCA LIMITS STUDY - 6.3 FOOT CASE
LOCAL OXIDATION

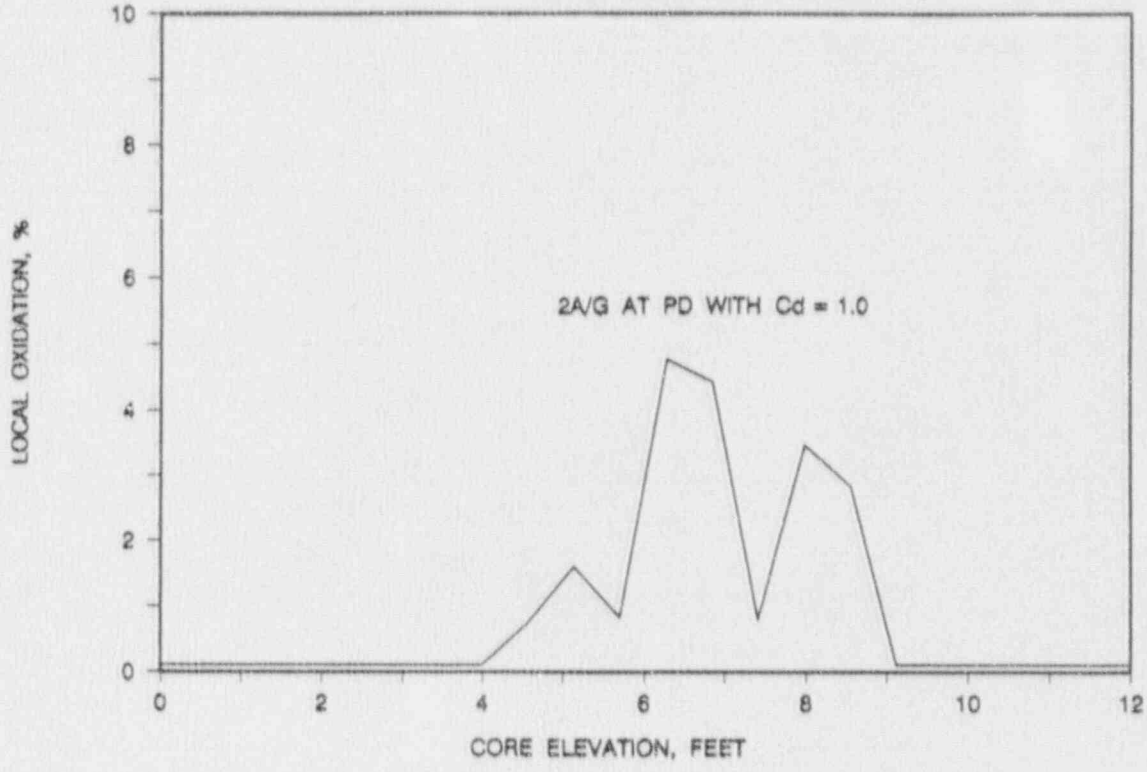

FIGURE 8-16 LOCA LIMITS STUDY - 8.0 FOOT CASE
MASS FLUX DURING BLOWDOWN AT PEAK POWER LOCATION

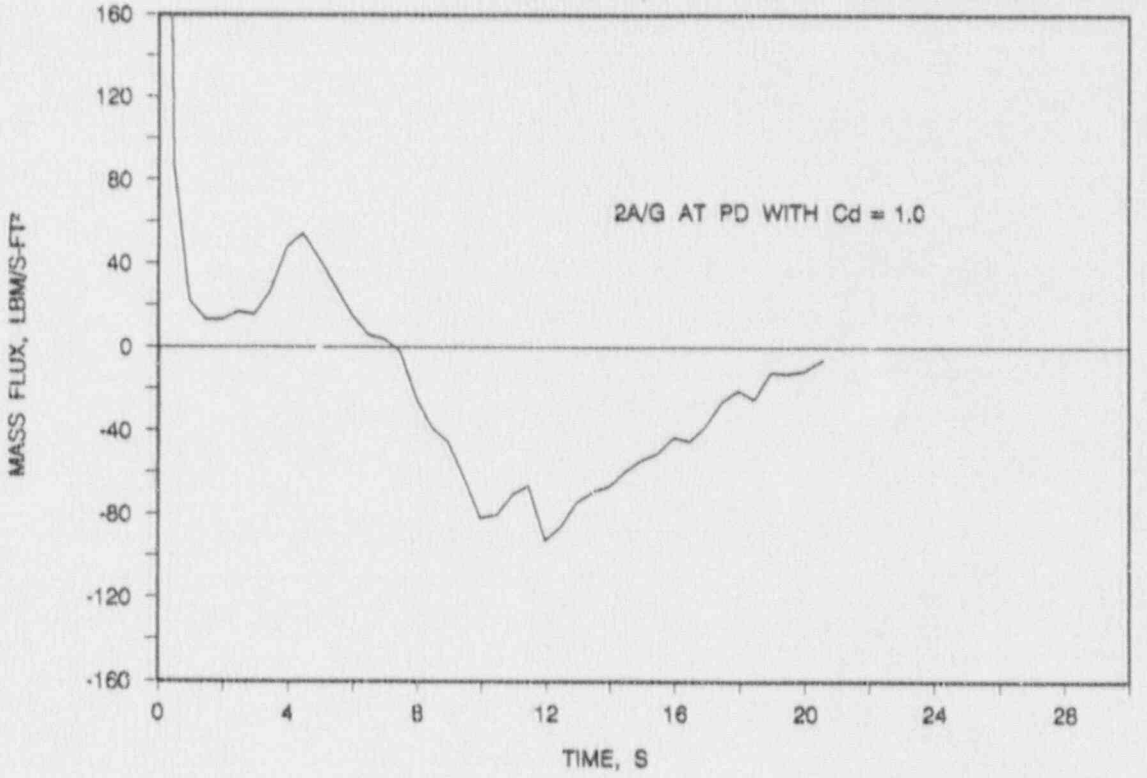

FIGURE 8-17 LOCA LIMITS STUDY - 8.0 FOOT CASE
CLADDING TEMPERATURES

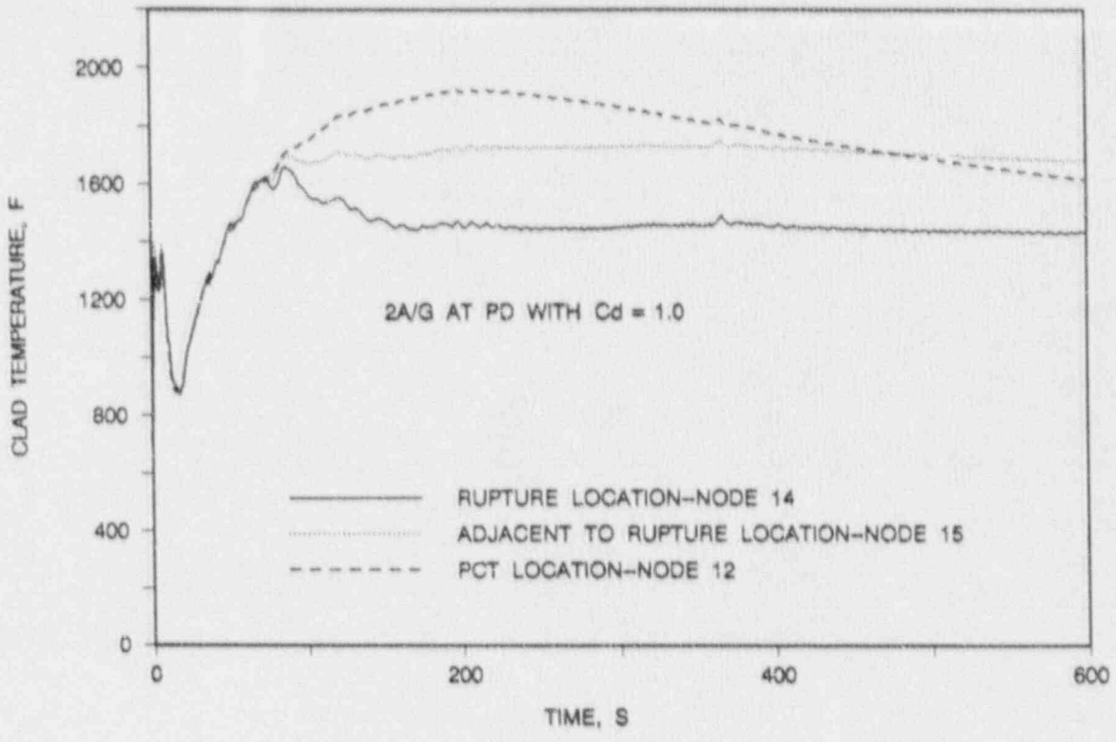

FIGURE 8-18 LOCA LIMITS STUDY - 8.0 FOOT CASE
HEAT TRANSFER COEFFICIENT AT PCT LOCATION

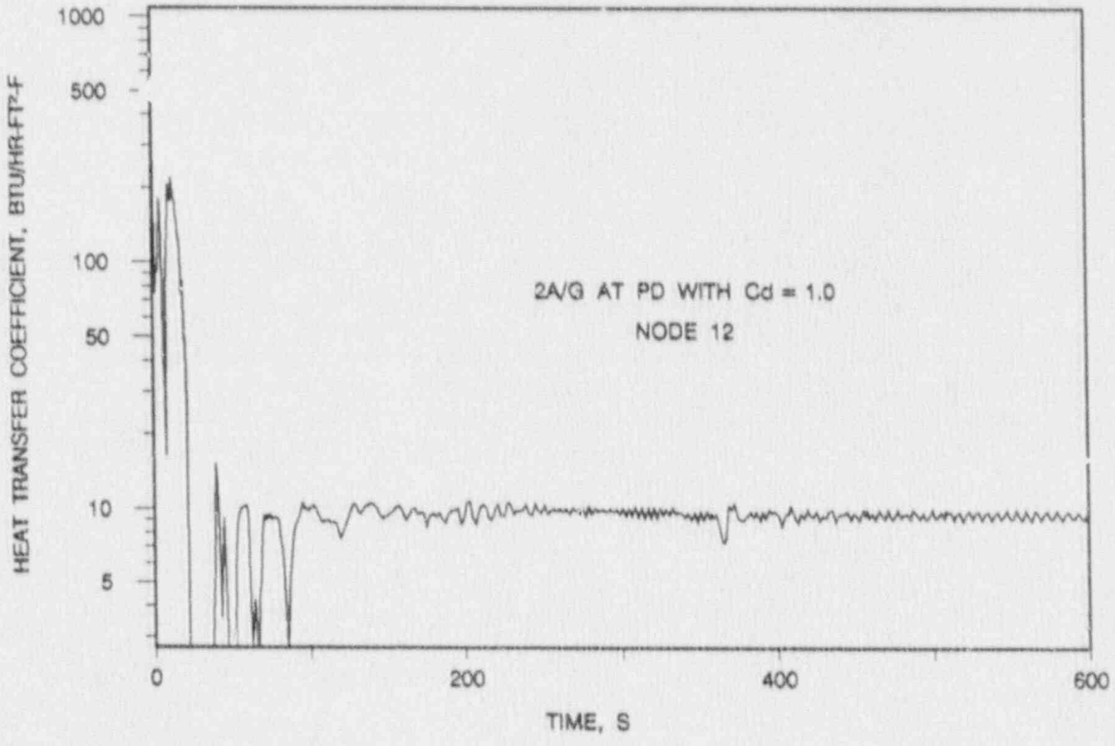

FIGURE 8-19 LOCA LIMITS STUDY - 8.0 FOOT CASE
LOCAL OXIDATION

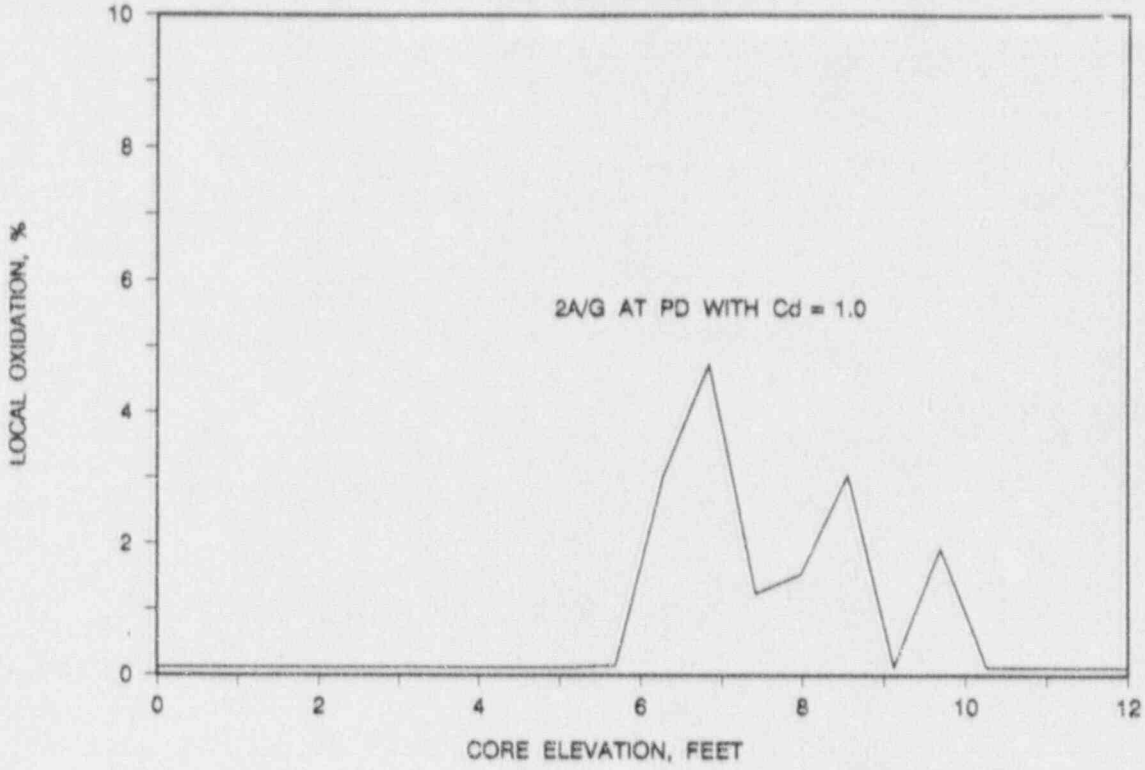

FIGURE 8-20 LOCA LIMITS STUDY - 9.7 FOOT CASE
MASS FLUX DURING BLOWDOWN AT PEAK POWER LOCATION

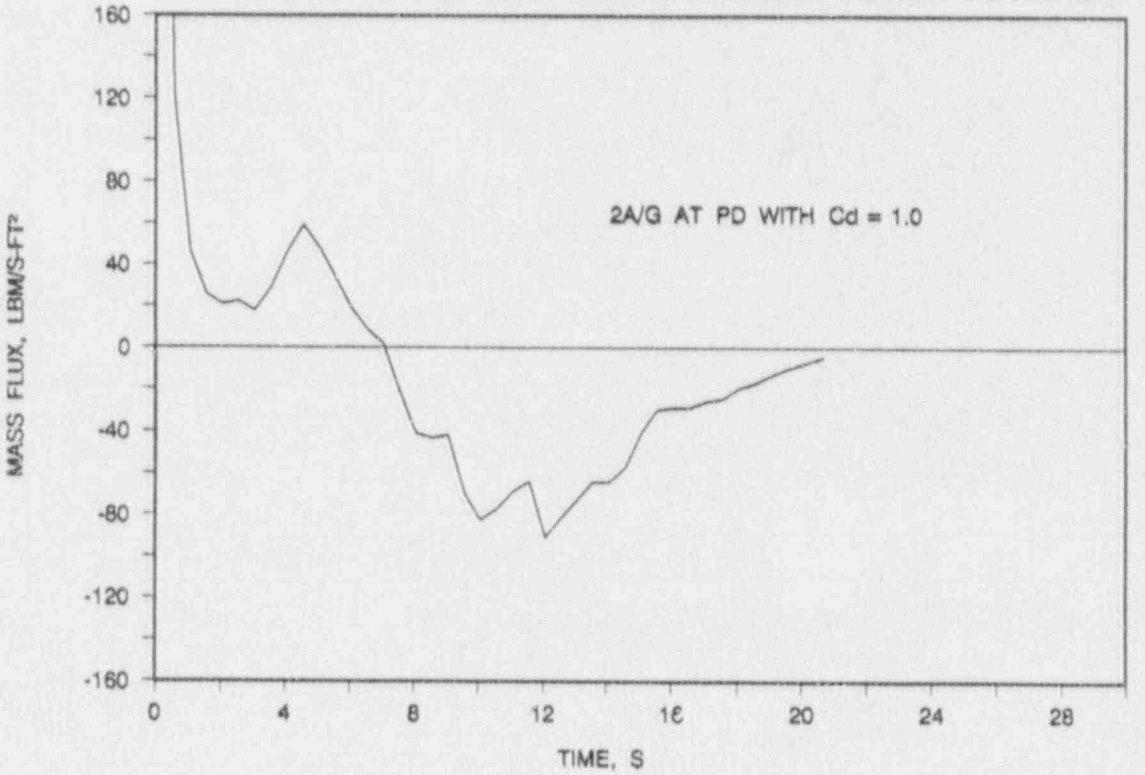

FIGURE 8-21 LOCA LIMITS STUDY - 9.7 FOOT CASE
CLADDING TEMPERATURES

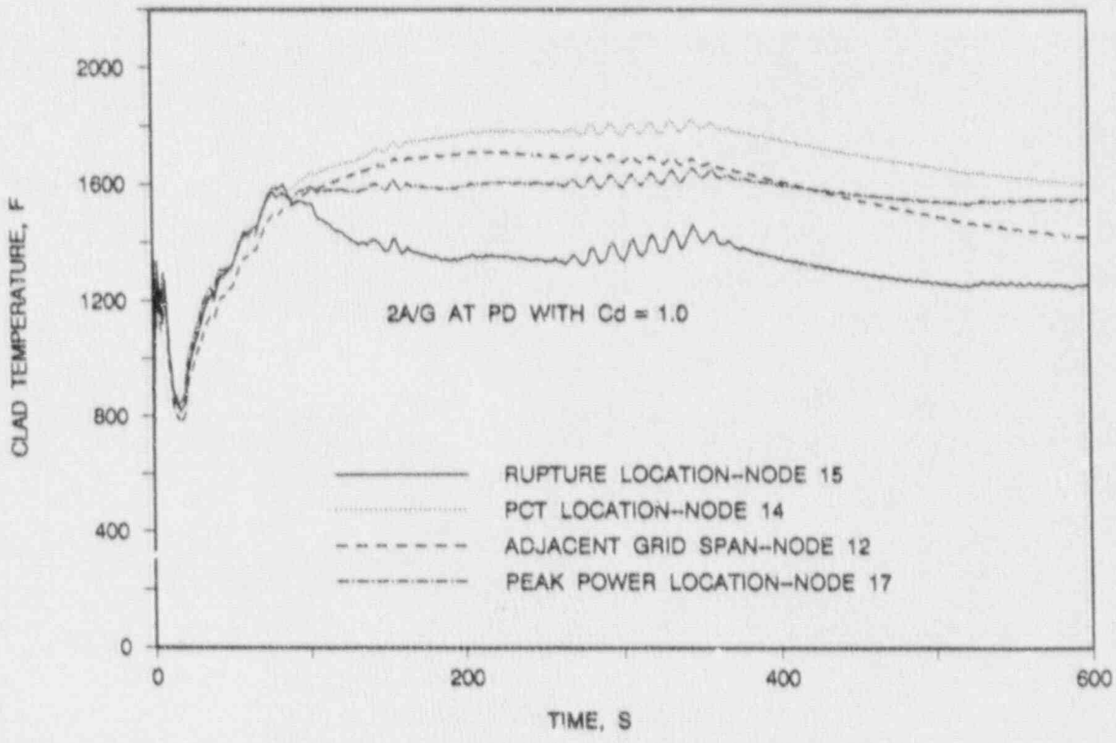

FIGURE 8-22 LOCA LIMITS STUDY - 9.7 FOOT CASE
HEAT TRANSFER COEFFICIENT AT PCT LOCATION

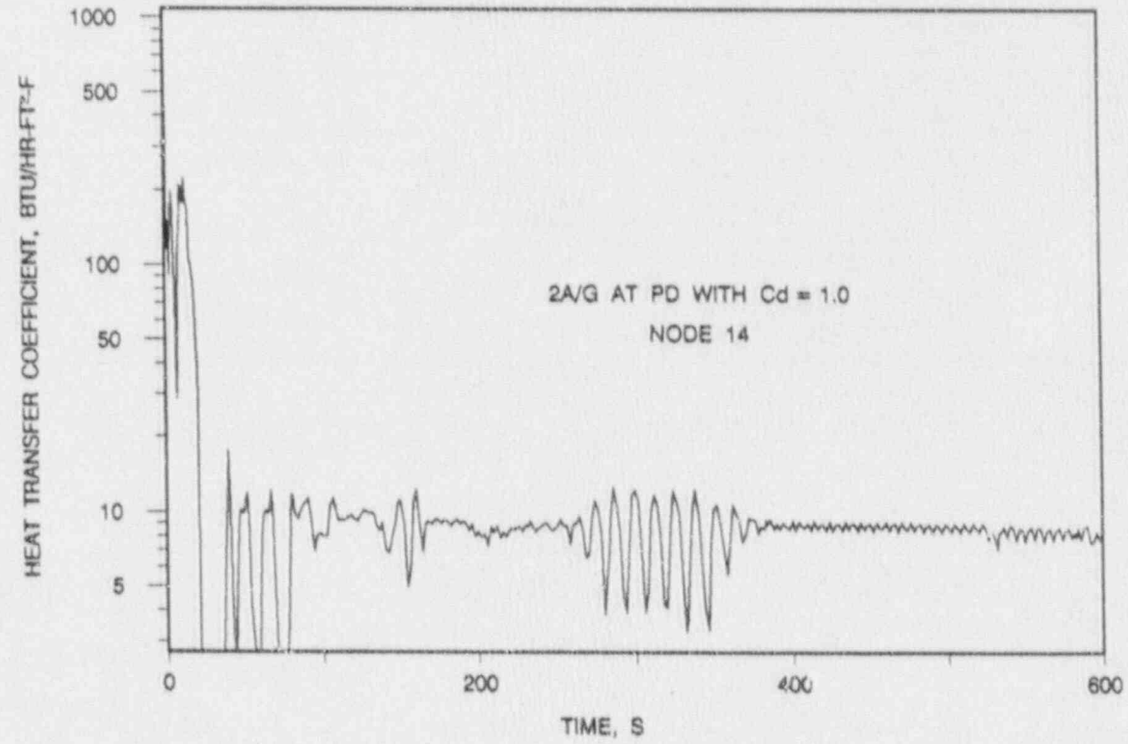

9. Whole-Core Oxidation and Hydrogen Generation

The third criterion of 10 CFR 50.46 states that the calculated total amount of hydrogen generated from the chemical reaction of the cladding with water or steam shall not exceed 0.01 times the hypothetical amount that would be generated if all of the metal in the cladding cylinders surrounding the fuel, excluding the cladding surrounding the plenum volume, were to react. The method provided in the BWFC evaluation model, Reference 1, has been applied to determine corewide oxidation for each of the LOCA limits cases. In the calculations, local cladding oxidation was computed as long as the cladding temperature remained above 1500 F, and the REFLOD3B analysis did not show that the cladding was within the core flooded region. The flooded region of the core was conservatively taken to be twenty percent above the core collapsed liquid level. These local oxidations are summed over the core to give the core-wide oxidation. The figures in Chapter 8 give the local oxidation for the hot pin including the initial oxide layer. The only difference between these distributions and the ones used for the whole core calculation is that the initial oxide layer is subtracted before the integration in order to provide a measure of the hydrogen produced during the LOCA. The results of these calculations for each of the power distributions of the LOCA Limits cases are:

Case	Whole Core Oxidation, %
...?-ft Peak	0.25
4.6-ft Peak	0.41[1]
6.3-ft Peak	0.40
8.0-ft Peak	0.32
9.7-ft Peak	0.29[2]

[1] See the response to question number 13 on BAW-10174.

[2] The 9.7' case has been reanalyzed at a higher F_q and the results of the analysis are reported in Appendix B.

Because these cases represent a range of the possible power distributions that can occur in the plant, the maximum possible oxidation that can occur during a LOCA at the McGuire or Catawba plants is calculated to be less than 0.41 percent. Thus, the third criterion of 10 CFR 50.46, which limits the reaction to 1 percent or less, is met with considerable margin.

assemblies differ in the following areas: unrecoverable pressure drops across the assemblies, initial fuel temperatures, initial pin internal gas pressure, and the axial power profile. The impact of each of these items, with respect to the controlling aspects of the SBLOCA transient, will be evaluated in the following paragraphs.

Mark-BW fuel assemblies have unrecoverable pressure drops that are approximately 1 psi lower than those of the Westinghouse OFA assemblies. The associated effect in overall loop pressure drop would translate to less than 1 percent difference in the initial forced flow. At the same steady-state core power and effectively identical loop flows, the controlling hot leg initial temperature is also essentially unaffected. The maximum hot leg temperature variation will be less than 1 F. Thus, the initial subcooled depressurization phase of the SBLOCA will be unaltered. The reactor trip signal and pump trips will occur at the same time in the transient as in the reference FSAR calculations.

The impact of the fuel bundle resistance will be even less during the pump coastdown and natural circulation phase because the flows during this phase are much reduced. Significant margins exist such that CHF will not be exceeded. All of the initial stored energy in the fuel will still be transferred to and removed by the steam generators. Therefore, core resistance variations will not change the fuel thermal transient or impact the existing evaluations.

Changes in the initial fuel temperature add or subtract overall energy from the RCS. The initial fuel energy is removed from the fuel pin during the reactor coolant pump coastdown phase and rejected from the system via the steam generators. Therefore, the initial fuel enthalpy of operation has virtually no impact

beyond the loop coastdown period. The core energy content during the loop draining and boil-off mode will be identical to the current licensing base.

The fuel pin internal gas fill pressures are similar to the Westinghouse values, but may differ slightly. The internal gas pressure could affect the fuel/cladding gap dimensions and rupture time. During the initial phase of the accident however, the fuel temperatures approach the system saturation temperature within a fraction of a minute following reactor trip and the impact of gap differences is negligible. During the core boil down phase the timing of rupture could differ slightly. The Mark-BW fuel pin has a larger internal gas volume, a slightly larger fuel volume, and a slightly higher fill gas pressure than the OFA. Because of the higher fill gas pressure the Mark-BW fuel will have a slightly higher internal pressure at beginning-of-life conditions. However, because of the larger gas volume available the Mark-BW pressurization with burnup will be slower than the OFA's. At burnups for which a rupture is possible during SBLOCA, the OFA fuel pin is higher in pressure than the Mark-BW. The difference, although very small, would tend to delay the rupture of the Mark-BW over the OFA. However, since the SBLOCA temperatures peak at approximately 1500 F, the impact of a difference in rupture timing on the resultant peak cladding temperature is negligible.

As a final point, SBLOCA imposed plant operating limits, including maximum allowable total peaking, will not be altered due to the use of BWFC-supplied fuel. Thus, the axial power profile used by Westinghouse in the SBLOCA analyses remains bounding. This assures that the thermal load imposed on the fuel during a temperature excursion remains conservatively modeled. The thermal results, cladding temperatures, for the present FSAR evaluations are, therefore, conservative for Mark-BW fuel.

In summary, the core resistance variations will not affect the loop flows such that the controlling hot leg temperature or CHF points are altered. The steam generator heat removal rate during the flow coastdown period will compensate for any initial fuel stored energy fluctuations. All controlling parameters in the phases following the pump coastdown and natural circulation phase will be unchanged. Therefore, since the overall RCS geometry, initial operating conditions, licensed power, and governing phenomena are effectively unchanged, the existing FSAR calculations should remain bounding for operation of the Catawba and McGuire units with BWFC-supplied fuel.

12.3 Current FSAR Results

The Westinghouse calculations of SBLOCA accidents for the McGuire and Catawba units are not the limiting LOCAs as predicted by the NOTRUMP and LOCTA-IV computer codes. The calculated results documented in the current McGuire and Catawba FSARs predict peak SBLOCA cladding temperatures less than 1500 F. All parameters are well within the acceptance criteria limits of 10 CFR 50.46. Even wide variations in SBLOCA results would not cause the SBLOCA to be limiting. Thus, considerable margins exist such that variations in the SBLOCA results would not alter either the plant technical specifications or operating procedures.

12.4 Compliance with Acceptance Criteria

The existing SBLOCA calculations contained in the McGuire and Catawba FSARs are valid and bounding for the BWFC Mark-BW fuel. The reactor coolant system, decay heat levels, and other system controlling parameters remain unchanged by the reload fuel. A significant safety margin exists between the calculated results and 10 CFR 50.46 limits. The fuel design differences between the Westinghouse OFA and the BWFC Mark-BW do not substantially alter

the results of SBLOCA evaluations. Adequate core cooling has already been demonstrated and does not need to be repeated because of the change in fuel design. The present SBLOCA evaluation calculations remain valid for the McGuire and Catawba fuel reloads supplied by BWFC. These analyses remain the small break evaluations of record for demonstrating compliance with the criteria of 10 CFR 50.46.

Appendix B. Fq Increase--9.7' LOCA Limits Case

[THIS APPENDIX WAS ADDED IN ITS ENTIRETY IN REVISION 1 OF BAW-10174, DATED NOVEMBER 1990.]

The analysis of the 9.7' LOCA limits case reported in Chapter 8 was based on a total peaking factor, F_q, of 2.1, as shown in Figure 8-1. This appendix presents the results of a reanalysis of the 9.7' case at a total peak of 2.23, an increase of 0.13 from the original calculation reported in Chapter 8. The updated total peaking factor curve, which replaces that presented in Figure 8-1 as an LBLOCA limit on plant operation, is shown in Figure B-1. The total peaking burnup adjustment factor curve shown in Figure 8-2 remains unchanged and applies to the peaking factors in Figure B-1. Radial peaking was maintained at 1.55 in the reanalysis, and the revised axial power profile is presented in Figure B-2.

The results presented in this appendix are based on two methodology modifications not in the Chapter 8 work. First, the Chapter 8 analyses were based on BEACH Version 10.0. During the licensing review of BAW-10174, BWFC discovered code errors in the BEACH Version 10.0 gap heat transfer logic. The errors were corrected in BEACH Version 11.0 and reported to the NRC in the response to question number 5 on BAW-10166 (BEACH), Revision 2. (NRC has approved the use of BEACH Version 11.0 in their August 13, 1990 SER on the BEACH topical report, BAW-10166.) The impact of the code errors on Chapter 8 results was assessed in the response to question number 30 on BAW-10174, and found not to produce substantial changes in PCT. Secondly, in response to question number 2 on BAW-10168, Revision 1, BWFC revised its metal-water reaction methodology from a 1500 F to a 1000 F

threshold temperature. The impact of the change on the results reported in Chapter 8 was assessed in the response to question number 13 on BAW-10174, and was found to produce small changes in results and to maintain significant margins to 10CFR50.46 limits. The update 9.7' case described in this appendix used BEACH Version 11.0 and the upgraded metal-water reaction methodology.

Figures B-3 through B-6 presents the results of the 9.7' case reanalysis, and Table B-1 presents a comparison between the original and revised cases. Basic trends between the original and revised cases remain unchanged. The PCT increased only 19 F from 1823 F to 1842 F. Peak local oxidation changed from 3.7 percent to 3.4 percent, while whole core oxidation increased from 0.29 percent to 0.44 percent. The decrease in the peak local oxidation percentage is a direct result of using the quench front to terminate oxidation. For the original case oxidation was terminated based on 120 percent of the core collapsed water level, whereas the revised analysis used the REFLOD3B predicted quench height. Comparing quench front advancement and 120 percent of the collapsed water level, on an elevation versus time plot, shows that, above a core height of about eight feet, the quench front curve predicts an earlier quench time than does the collapsed water level curve. Based on the responses to questions 13 and 30 on BAW-10174, the 4.6' LOCA limits case will still remain limiting with respect to PCT and clad oxidation percentage.

The reanalysis of the 9.7' LOCA limits case resulted in a peak clad temperature of 1842 F, and local and whole core oxidation percentages of 3.4 percent and 0.44 percent, respectively. Core geometry (Chapter 10) and long-term cooling (Chapter 11) are not impacted by the reanalysis. Thus, compliance with the five criteria of 10CFR50.46 has been demonstrated.

Table B-1 LOCA Limits Results--Updated 9.7' Case

	9.7' Location of Peak Power	
Item or Parameter	Original	Updated
End-of-Blowdown, s	20.8	21.0
Liquid in Reactor Vessel at EOB, ft^3	79.0	83.7
Bottom-of-Core Recovery, s	32.9	33.1
Time of Rupture, s	84.4	84.1
Ruptured Node *	15	15
PCT at Rupture Node, F	1602	1604
Oxide at Rupture Node, %	0.8	1.1
Node Adjacent to Rupture *	14	14
PCT of Adjacent Node, F	1823	1842
Oxide at Adjacent Node, %	3.2	3.4
Node in Adjacent Grid Span *	12	12
PCT of Adjacent Grid Span, F	1718	1700
Oxide at Adjacent Grid Span, %	2.0	0.6
Pin PCT Node *	14	14
Peak Local Oxidation, %	3.7	3.4
Whole Core Oxidation, %	0.29	0.44

* Refer to Figure 4-4 for noding arrangement.

FIGURE B-1 AXIAL DEPENDENCE OF ALLOWED TOTAL PEAKING FACTOR
LARGE BREAK LOCA MARK-BW, UPDATED 9.7 FOOT CASE

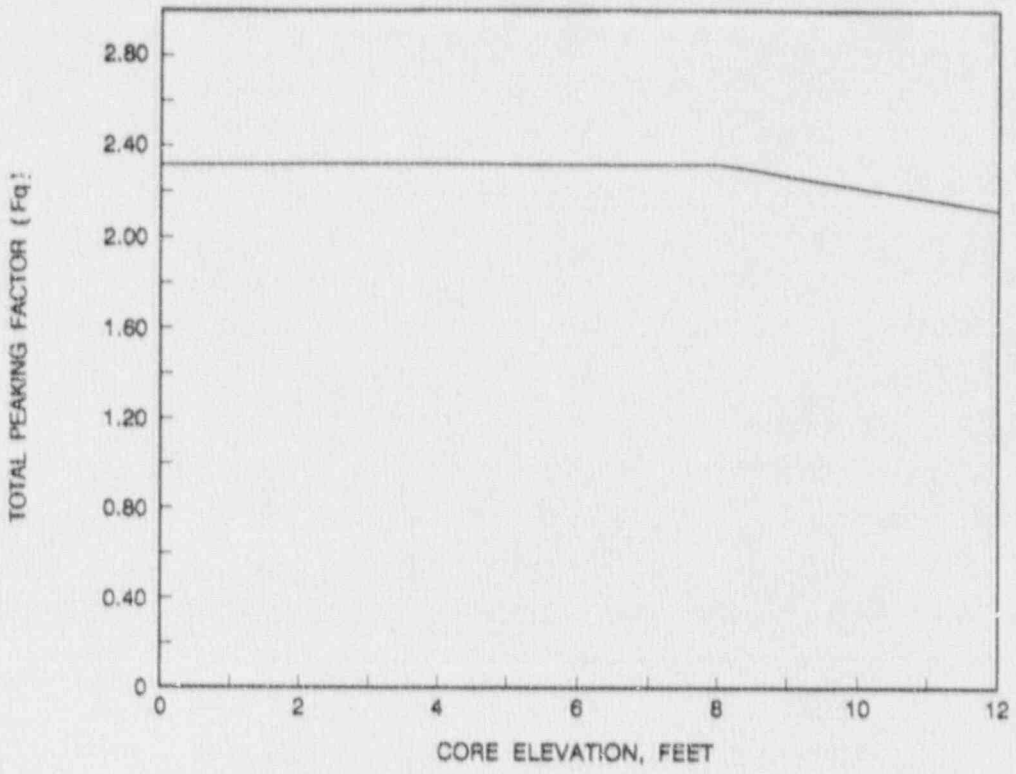

FIGURE B-2 LOCA LIMIT STUDY - AXIAL POWER SHAPE
UPDATED 9.7 FOOT CASE

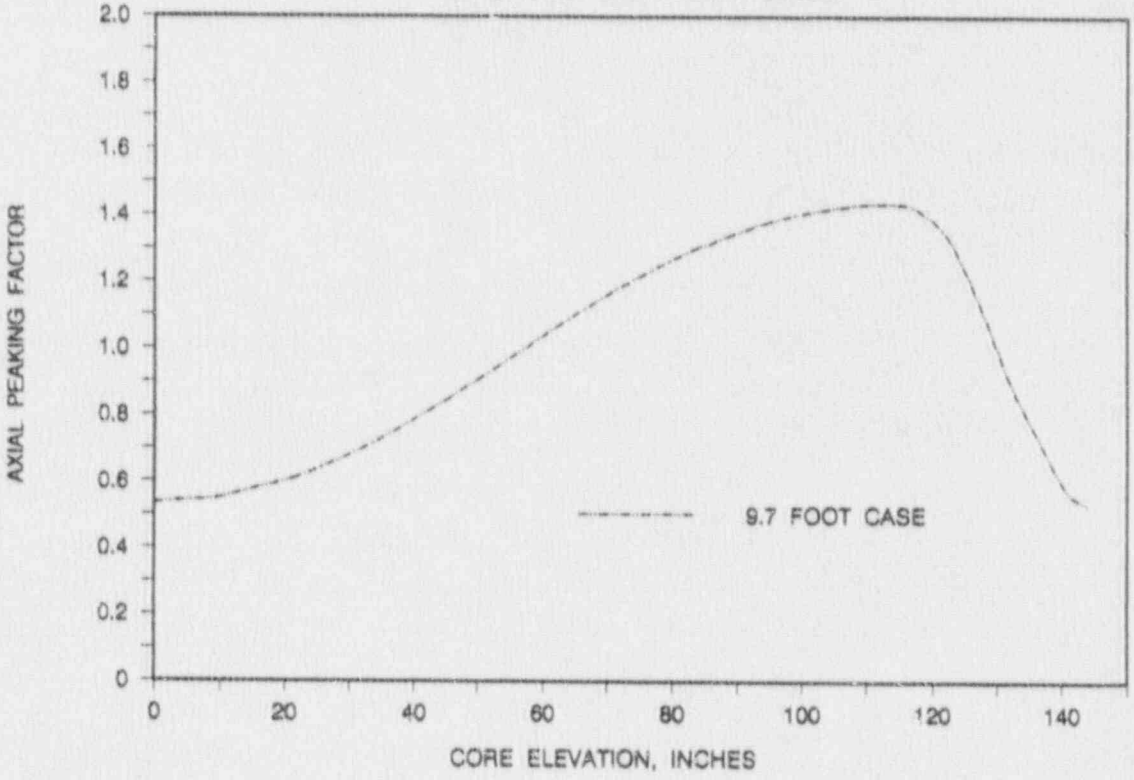

FIGURE B-3 LOCA LIMITS STUDY - UPDATED 9.7 FOOT CASE
MASS FLUX DURING BLOWDOWN AT PEAK POWER LOCATION

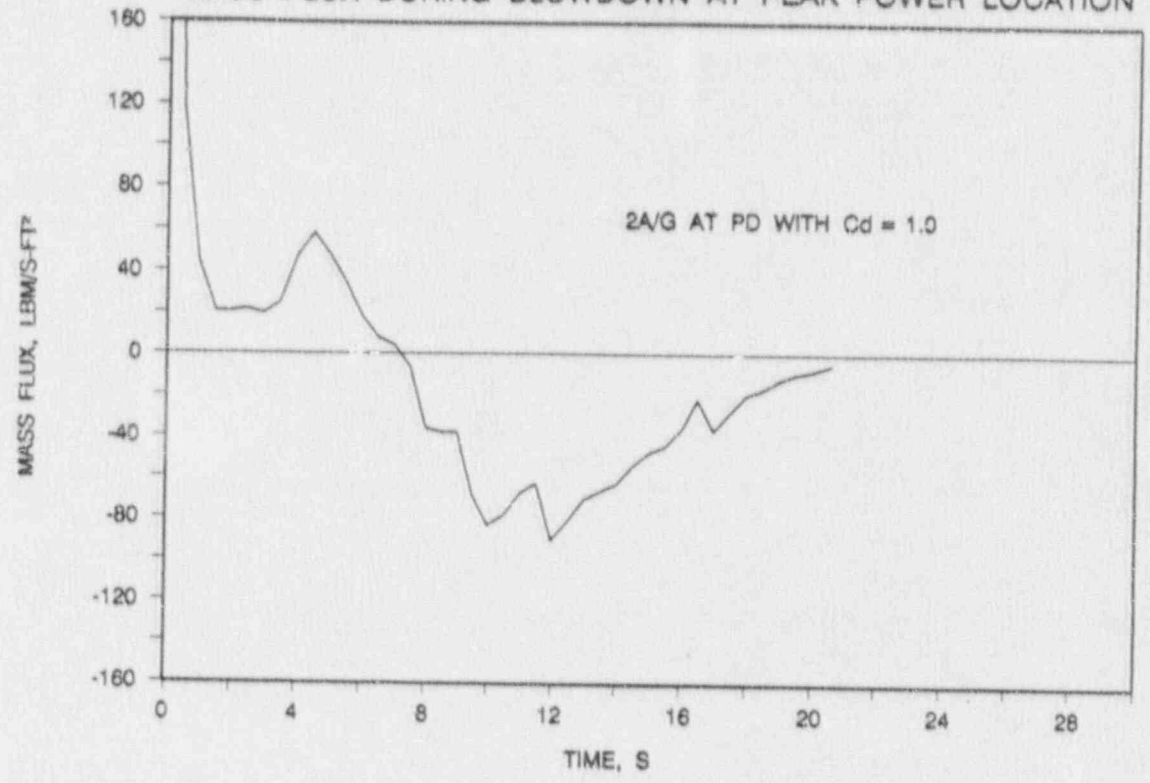

FIGURE B-4 LOCA LIMITS STUDY - UPDATED 9.7 FOOT CASE
CLADDING TEMPERATURES

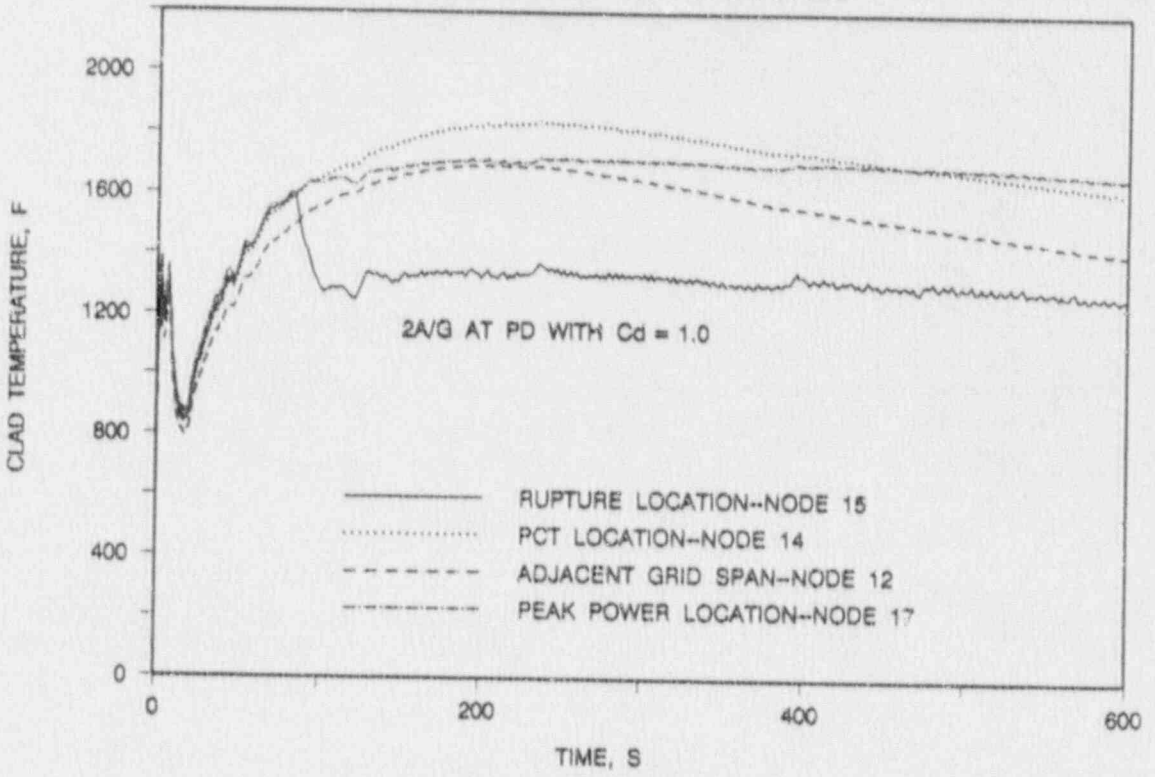

FIGURE B-5 LOCA LIMITS STUDY - UPDATED 9.7 FOOT CASE
HEAT TRANSFER COEFFICIENT AT PCT LOCATION

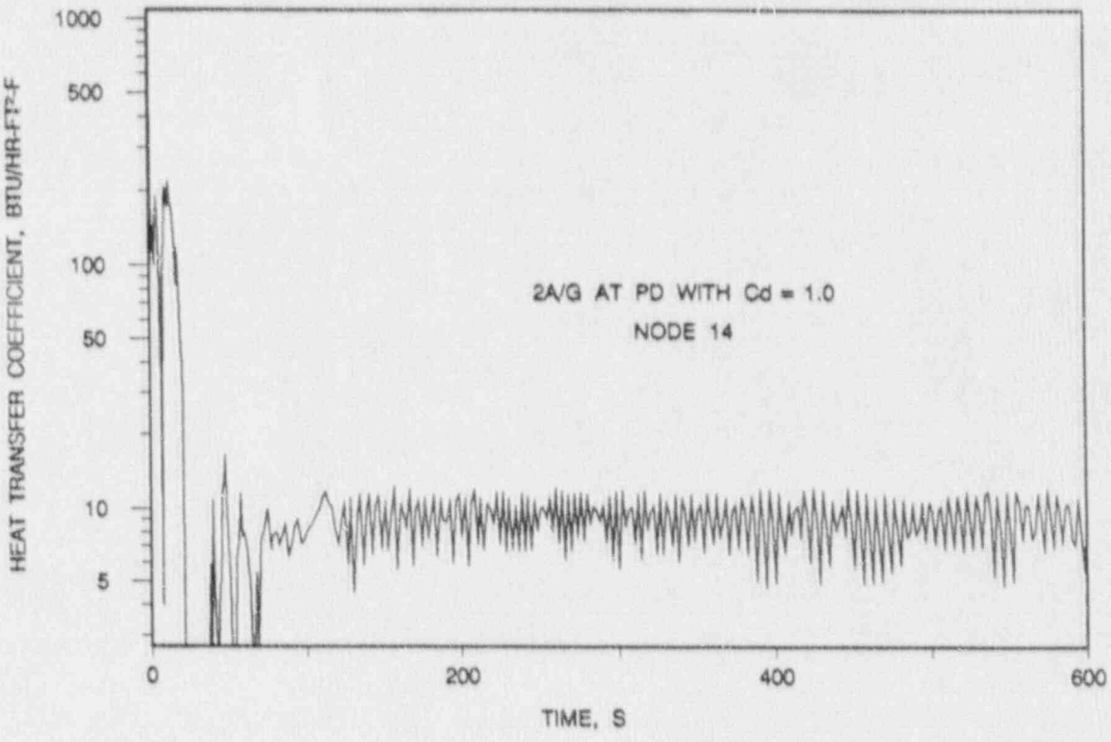

FIGURE B-6 LOCA LIMITS STUDY - UPDATED 9.7 FOOT CASE
LOCAL OXIDATION